General Thoracic and Cardiovascular Surgery (2022) 70:445–454
https://doi.org/10.1007/s11748-021-01725-y

ORIGINAL ARTICLE

Translational model of vein graft failure following coronary artery bypass graft in atherosclerotic microswine

Mohamed M. Radwan[1,2] · Aleem Siddique[3] · Finosh G. Thankam[1,2] · Kouassi Tata Kouassi[2] · Devendra K. Agrawal[1,2]

Received: 27 November 2020 / Accepted: 20 October 2021 / Published online: 26 October 2021

Abstract

Objective Vein graft failure is a major complication following coronary artery bypass graft surgery. There is no translational model to understand the molecular mechanisms underlying vein-graft failure. We established a clinically relevant bypass graft model to investigate the underlying pathophysiological mechanisms of vein-graft failure and identify molecular targets for novel therapies.

Methods Six female Yucatan microswine fed with high cholesterol diet underwent off-pump bypass, using superficial epigastric vein graft, which was anastomosed to an internal mammary artery and distal left anterior descending artery. Vein-graft patency was examined 10-months after bypass surgery by echocardiography, coronary angiography, and optical coherence tomography followed by euthanasia. Coronary tissues were collected for histomorphometry studies.

Results Atherosclerotic microswine were highly susceptible to sudden ventricular fibrillation with any cardiac intervention. Two out of six animals died during surgery due to ventricular fibrillation. Selection of the anesthetics and titration of their doses with careful use of inotropic drugs were the key to successful swine cardiac anesthesia. The hypotensive effects of amiodarone and the incidence of arrhythmia were avoided by the administration of magnesium sulfate. The vein-graft control tissue displayed intact endothelium with well-organized medial layer. The grafted vessels revealed complete occlusion and were covered with fibrous tissues. Expression of CD31 in the graft was irregular as the layers were not clearly defined due to fibrosis.

Conclusion This model represents the clinical vein-graft failure and offers a novel platform to investigate the underlying molecular mechanisms of vein-graft disease and investigate novel therapeutic approaches to prevent its progression.

Keywords Coronary heart disease · Coronary artery bypass surgery · Animal model · Vein-graft failure · Cardiovascular diseases · Translational cardiology

Abbreviations

ABGS	Arterial blood gases
ACS	Activated clotted time
CABG	Coronary artery bypass graft
CRT	Capillary refill time
EKG	Electrocardiogram
$ETCO_2$	End tidal CO_2
HDL	High density lipoprotein
HFD	High fat diet
IMA	Internal mammary artery
LAD	Left anterior descending artery
LDL	Low density lipoprotein
OCT	Optical coherence tomography
SEV	Superficial epigastric vein
TG	Triglycerides

✉ Devendra K. Agrawal
DAgrawal@WesternU.edu

[1] Department of Translational Research, Western University of Health Sciences, Pomona, CA 91766, USA

[2] Department of Clinical and Translational Science, Creighton University School of Medicine, Omaha, NE 68178, USA

[3] Division of Cardiothoracic Surgery, University of Nebraska Medical Center, Omaha, NE 68198, USA

Introduction

The success of coronary artery bypass graft (CABG) surgery largely depends on the patency of the vascular graft. Although CABG surgery incurs short-term risks, it is associated with an overall increase in the long-term median

survival rates [1–3]. Although the short-term patency of the vascular conduits is excellent, the long-term patency rates are not favorable [4–7]. Several arterial and venous grafts have been utilized, and they revealed variable and vessel-specific outcomes. Venous graft failure has been attributed to trauma, hemodynamic factors, thrombosis, intimal hyperplasia and atherosclerosis [4–11]. Better understanding of the underlying basic molecular mechanisms associated with venous graft failure is a prerequisite for developing novel approaches to improve graft patency.

The objective of the study was to establish a large animal model of CABG, which simulates the biochemical and pathological aspects in human coronary artery disease (CAD). This clinically relevant model used venous graft analogous to the great saphenous vein used as a conduit in human CABG. It offers strategies to overcome the challenges of cardiac anesthesia and CABG surgery in pigs. The successful swine model of CABG using superficial epigastric vein (SEV) as a free graft described in this study sets the stage to unravel the cellular and molecular mechanisms of vein graft disease and to explore the novel molecular targets to prevent venous graft failure and improve its patency. This would improve CABG surgery outcome and avoid the need for re-surgery, helping millions of CAD patients nationally and internationally.

Materials and methods

Animals

All animal procedures for this research were performed according to NIH, OLAW and USDA guidelines and obtained prior approval from the IACUC of Creighton University (IACUC protocols #0963 and #1052). Six 8–10 months old female Yucatan microswine (*Sus scorfa)*, purchased from Sinclair BioResources, were recruited to the study. They had blood tests while on a normal swine diet, before feeding high fat high cholesterol diet (pre-feeding blood tests). They were then fed with high fat high cholesterol (HFHC) diet, twice daily for 6–12 months.

The six microswine were fed a mixture of Teklad (Envigo, USA) swine high fat high cholesterol diet (HFHC) that consisted of 37.2% corn (8.5% protein), 23.5% soybean meal (44% protein), 5% alfalfa, 4% cholesterol, 4% peanut oil, 1.5% sodium cholate, and 1% lard; with the addition of 8% chocolate. Complete blood count, comprehensive metabolic panel (CMP) and blood lipid profile were performed pre- and post-feeding with the HFHC diet (Fig. 1).

Four domestic pigs were recruited as blood donors and euthanized after blood collection. In addition, prior to this study in Yucatan microswine, domestic pigs were subjected to SEV grafting between the ascending aorta and mid-left anterior descending coronary artery (LAD) as a proof of concept.

Preoperative preparations

The hypercholesterolemic Yucatan microswine were administered with aspirin 350 mg and clopidogrel (75 mg orally) for 2–3 days prior to surgery, and they fasted overnight. Four pints of whole blood were made available for blood transfusion during each CABG surgery. The animals were brought to the operating room, pre-anesthetized with acepromazine (1.1 mg/kg, SC) and 10 min later with ketamine (11–33 mg/kg, SC), and prepped for surgery.

Anesthesia

Anesthesia was induced with isoflurane gas (3–4% in oxygen). The animals were intubated, and two IV catheters (20–22 gauge) were inserted in the ear veins bilaterally. The anesthesia was maintained with isoflurane (1–2% in oxygen) throughout the procedure. Preemptive analgesic, prophylactic antibiotic, and prophylactic antiarrhythmic were administered. The animals were mechanically ventilated and closely monitored for mucous membrane color, capillary refill time (CRT), heart rate, rectal temperature, EKG, SPO_2, end tidal CO_2 ($ETCO_2$), arterial blood pressure

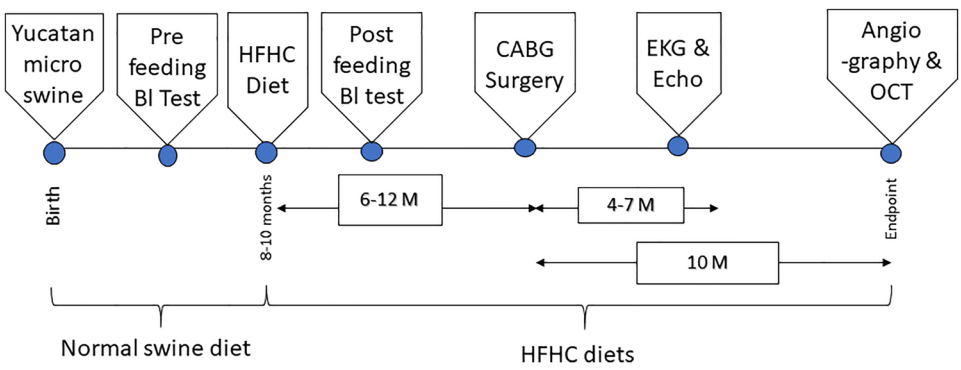

Fig. 1 Schematic diagram showing the study timeline of the procedures in all six Yucatan microswine

(noninvasive and invasive) and arterial blood gases (ABGS). Foley's catheter was inserted under aseptic conditions, for hourly urine output monitoring. The animals were covered with circulating warm water blankets to prevent hypothermia. Femoral arterial and venous lines were established for monitoring the arterial and central venous pressures, collecting serial blood samples for measuring ABGS and activated clotted time (ACT), and administering intravenous fluids and drugs when needed. After thoracotomy incision and attaining wound hemostasis, systemic heparin (100–200 IU/Kg IV) was administered and repeated, when necessary, to maintain ACT of 200 s throughout the CABG procedure. Phenylephrine 50–100 µg IV bolus was used to treat acute episodes of hypotension when the mean arterial blood pressure is ≤ 60 mmHg, and norepinephrine 8–12 µg/min IV infusion was used to attain systolic blood pressure of ≥ 90 mmHg at the time of distal anastomosis.

Histology and CD31 expression

The graft tissue was harvested post-sacrifice, placed in formalin, paraffin-embedded and sectioned using a microtome (5 µm thickness) histology and analysis of CD31 by immunofluorescence. The sections were deparaffinized for H&E and pentachrome staining following our previously reported protocol [12]. The stained slides were mounted using xylene-based mounting media and imaged at 20 × magnification.

The protein expression of CD31 was determined by the immunopositivity following our previously reported protocols [13, 14]. Briefly, the deparaffinized sections were subjected to rehydration, antigen retrieval, blocking (0.25% Triton X-100 and 5% horse serum in PBS) at room temperature for 90 min and incubation with primary antibody (1:300 dilution) specific to CD31 (Abcam Cat# ab28364). The fluorochrome-conjugated secondary antibody (1:400 dilution) was used to detect the primary antibody. Nuclei were counterstained with 4′,6-diamidino-2-phenylindole (DAPI) and imaged using the fluorescent slide scanner system (VS120-S6-W, Olympus).

Problems encountered during anesthesia

The synergistic effects of pre-anesthetic medications, isoflurane and amiodarone posed a substantial risk of severe intractable hypotension in pigs. In our experience, acepromazine (1.1 mg/kg IM/SC) and ketamine (11–33 mg/kg IM/SC) as pre-anesthetics, and 1–2% isoflurane in oxygen for maintenance had the least hypotensive effects compared to other drug combinations. However, judicious use of these drugs and titrating their doses to effect, in addition to careful use of inotropic drugs is the key for successful swine cardiac anesthesia. Swine are susceptible to sudden ventricular fibrillation with any cardiac intervention. Amiodarone (5–10 mg/kg, IV) as a loading dose over 15–20 min followed by 0.5–3.5 mg/kg/hour continuous rate IV infusion was used as prophylactic antiarrhythmic throughout the procedures to prevent ventricular fibrillation. We found it very effective if the amiodarone infusion was stopped 15–20 min before the distal anastomosis and replace it with magnesium sulfate (0.15–0.3 mEq/kg IV bolus) immediately before distal anastomosis to prevent the occurrence of arrhythmia and avoid the hypotensive effects of amiodarone during this critical step. Ultrasound-guided percutaneous cannulation of femoral vessels was adopted. In addition, we found it critical to start a whole blood transfusion when needed; the blood was collected from domestic pigs and was administered according to the estimated blood loss and the hematocrit value. The swine were monitored for transfusion reaction including skin rashes, fever, and tachycardia. Methylprednisolone (10–250 mg, IV), besides discontinuation of the blood transfusion, was prepared to administer with the first sign of transfusion reaction.

Harvesting superficial epigastric vein (SEV)

With the pig in the dorsal position under general anesthesia, a longitudinal skin incision approximately one-inch lateral to the mammary line was performed, after marking the vein position on the skin with the help of ultrasound. The SEV was gently dissected, and its branches were divided and clipped. SEV graft of about 10 cm was harvested and preserved in sterile heparinized saline solution. The skin incision was closed with a subcuticular absorbable suture.

Chest incision

Median sternotomy incision was performed followed by an incision of the pericardium to expose the heart with extreme care to avoid entering the pleural cavity; incision hemostasis was then achieved.

Coronary artery bypass graft (CABG)

Initially, 6 domestic swine had the free vein graft anastomosed to the ascending aorta proximally and the mid distal LAD distally which was ligated proximal to the anastomosis (Fig. 2), but due to the difficult exposure of the ascending aorta in swine, we opted to anastomosing the free SEV graft to the IMA proximally and the distal LAD distally as described below.

Briefly, the IMA was traced, mobilized and its distal end was ligated/clipped, the proximal anastomosis was performed by connecting the distal (caudal) end of the SEV graft to the IMA in end to side fashion, so the blood flows in the direction of the valves in the vein graft. The myocardium in the region of the distal anastomosis was

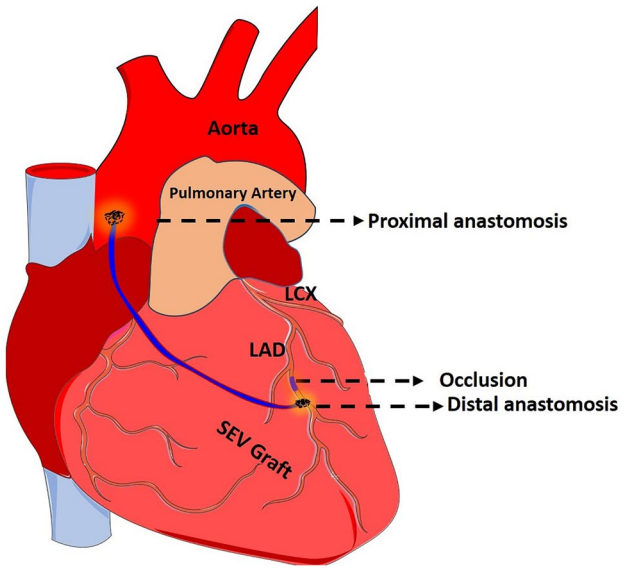

Fig. 2 Schematic illustration of the initial surgical approach in the domestic swine. SEV was used as the bypass graft conduit anastomosed proximally to the ascending aorta and distally to the LAD. This approach was used in all six Yucatan microswine

stabilized, using a cardiac surface stabilizing device. The left anterior descending (LAD) coronary artery was traced, the proposed region for distal anastomosis was exposed and prepped, with two silastic tapes (retract-o-tapes) looped around the vessel proximal and distal to the site of the anastomosis. The proximal (cranial) end of the SEV was then anastomosed to the side of the distal LAD using 7/0 prolene suture (end to side anastomosis). After completion of the anastomoses, the graft was examined for blood flow. The tape around the LAD proximal to the anastomosis was tightened temporarily to test the patency and efficiency of the anastomosis. The patency of the graft was confirmed by watching the myocardium supplied by the distal LAD for 10–15 min for color and contractility changes, and EKG tracing was monitored for evidence of arrhythmia or ischemic changes. After confirming the graft patency, the LAD proximal to the anastomosis was permanently occluded by 4/0 prolene ligature.

Chest drainage and closure of sternotomy incision

Briefly, a temporary sub-sternal chest tube was inserted through a separate stab incision. The sternotomy incision was closed using a stainless-steel suture and the skin with a subcuticular vicryl suture. The wounds were infiltrated with a long-acting local anesthetic. The substernal tube was removed once the animal became hemodynamically stable.

Postoperative management (supplementary methods)

Follow up and endpoint

The animals underwent EKG and Echocardiography at 4 and 7 months after the CABG procedure. Ten months after CABG, the animals underwent the terminal procedure (Fig. 1), which included, EKG, echocardiography, transfemoral coronary angiography and an attempt to perform vein graft angiography and optical coherence tomography (OCT).

Euthanasia

Euthanasia was performed by intravenous administration of a single dose of pentobarbital sodium (85 mg/kg) and phenytoin sodium (11 mg/kg). Swine were observed for the absence of heartbeat and respiration for 5 min prior to tissue harvest including the vein graft, coronary arteries, and ventricular wall specimens.

Statistical methods

The statistically significant difference in blood chemistry and other parameters between the groups was determined by unpaired '*t*' test with Welch's correction using GraphPad Prism software. The $P < 0.05$ values were considered significant.

Results

SEV was harvested and successfully anastomosed to the IMA and distal LAD in all six Yucatan microswine. Four animals survived the procedure (67%). Two pigs died on the operating table. Both developed ventricular fibrillation, one of them during performing the distal anastomosis and the other after removing the tourniquets upon completing the distal anastomosis. Both failed to respond to drug treatment and internal defibrillation. One animal (17%) developed myocardial depression and bradycardia after administration of the preanesthetic medications evidence by hypokinetic left ventricle on echocardiography. She was treated with inotropic drugs and atropine, allowed to recover from anesthesia, and operated later. No reaction to blood transfusion occurred in any of the animals.

All six Yucatan microswine developed hypercholesterolemia, as evidenced by significantly higher serum total and LDL cholesterol levels following gavage of high fat high cholesterol diet (post-feeding) compared to their levels during feeding with normal diet (pre-feeding) (Table 1).

The post-feeding complete metabolic and lipid panels showed significant changes in the serum glucose, alkaline

Table 1 Serum lipid profile parameters of experimental microswine pre- and post-feeding with high fat high cholesterol diet

Serum Constituent	Pre-HFD values, mg/dL	Post-HFD values, mg/dL	*P* value comparing pre- and post HFD
Total cholesterol	119.5 ± 16.4	469.2 ± 169.0	0.0037
LDL	55.2 ± 14.3	221.8 ± 64.4	0.0011
HDL	62.8 ± 5.5	95.8 ± 13.4	0.0006
TG	60.2 ± 25.7	64.7 ± 32.0	0.7942

HFD high fat high cholesterol diet, *HDL* high density lipoprotein, *LDL* low-density lipoprotein, *TG* triglycerides, The statistically significant difference between the groups was determined by unpaired '*t*' test with Welch's correction using GraphPad Prism software. $N = 4$; The $P < 0.05$ values were considered significant

Table 2 Complete blood count and a complete metabolic panel of experimental microswine pre- and post-feeding with high fat high cholesterol diet

Blood/serum parameter	Pre-HFD value	Post-HFD value	*P* value
WBC (10^3/μL)	14.3 ± 3.7	13 ± 2.0	0.4381
RBC (10^6/μL)	7.2 ± 0.4	7.6 ± 0.5	0.1125
HgB (g/dL)	14.2 ± 1.3	14.6 ± 0.9	0.5631
HCT (%)	44.0 ± 4.3	47 ± 2.2	0.1715
PLT (10^3/μL)	500.8 ± 140.2	617.7 ± 94.4	0.1257
BUN (mg/dL)	19.5 ± 3.2	15.7 ± 2.9	0.0567
CRE (mg/dL)	0.8 ± 0.1	0.8 ± 0.1	0.8153
GLU (mg/dL)	95.2 ± 7.5	79.0 ± 5.6	0.0021
Na (mEq/L)	144.0 ± 6.2	142.2 ± 3.2	0.5369
K (mEq/L)	5.6 ± 0.8	5.9 ± 0.3	0.3542
Cl (mEq/L)	99.5 ± 2.7	102.0 ± 2.4	0.1169
ALP (U/L)	92.8 ± 6.9	255.8 ± 42.7	0.0002
ALT (U/L)	40.2 ± 8.3	87.8 ± 72.2	0.1675
AST (U/L)	35.0 ± 9.6	119.8 ± 149.1	0.2224
TBIL (mg/dL)	0.1 ± 0.0	0.1 ± 0	0.3632
TP (g/dL)	6.5 ± 0.7	7.1 ± 0.3	0.0954
ALB (g/dL)	3.8 ± 0.4	3.7 ± 0.4	0.6424
GLOB (g/dL)	2.7 ± 0.4	3.5 ± 3.5	0.0035
A\G ratio	1.4 ± 0.2	1.0 ± 0.1	0.0026
Ca (mg/dL)	11.0 ± 0.8	10.9 ± 0.3	0.827
PHOS (mg/dL)	7.9 ± 0.5	7.8 ± 0.7	0.883

The statistically significant difference between the groups was determined by unpaired '*t*' test with Welch's correction using GraphPad Prism software. $N = 4$; The $P < 0.05$ values were considered significant

phosphatase, globulin levels, A:G ratio, compared to the pre-feeding panels, while there were no significant changes in the post-feeding complete blood count or serum electrolytes including serum calcium compared to the pre-feeding parameters (Table 2). The serum total cholesterol levels of the six swine which had an ascending aorta to LAD anastomosis early in the project, ranged between 60 and 82 mg/dL at the time of CABG surgery. All the Yucatan microswine which survived the procedure had normal wound healing and regained their normal activities within 10–14 days after CABG surgery. At the time of euthanasia, 10 months after CABG surgery, the SEV graft of these 4 animals was completely or partially occluded. Out of the first cohort of six domestic swine, which had ascending aorta to LAD anastomosis, two (17%) survived the procedures had angiography (Fig. 3) and euthanized two months following the CABG surgery.

The H and E and pentachrome (Figs. 4 and 5) staining of the grafted vessels revealed complete occlusion and was covered with fibrous tissues. The SEV control tissue displayed intact endothelium with well-organized medial layer whereas the graft was completely occluded with fibrous tissue adhesions as evident by the increased collagen staining. The ECM disorganization was observed in the graft as displayed by the wavy appearance of ECM fibers with a concomitant increase in elastic tissue. The occluded lumen was infiltrated with vascular smooth muscle cells in the subendothelial layer (superficial to the disrupted internal elastic membrane) showing the neointimal formation and proliferative smooth muscle cells migrated from the tunica media through the disrupted internal elastic membrane. In addition, the expression of endothelial biomarker CD31 was evident in the graft tissue and SEV control (Fig. 6). However, the expression of CD31 in the graft was irregular as the layers were not clearly defined due to fibrosis. Importantly, the presence of CD31 signifies the existence of vascular tissue remnants in the occluded graft.

Discussion

We present SEV as a novel vein graft, as it has the advantages of relative ease to harvest, greater diameter than the swine saphenous veins, which are two small venous channels associated with the saphenous artery on the medial side of the thigh and communicate with each other via multiple small communicating branches. The SEV is analogous to the human great saphenous vein and has minimal post-harvest complications [15–20]. SEV was not previously reported in swine CABG models, however, it has been used in the rat model as an interposition graft to study vein graft disease [21, 22]. The overall approach for this protocol is depicted in Fig. 7. We successfully performed survival CABG surgery

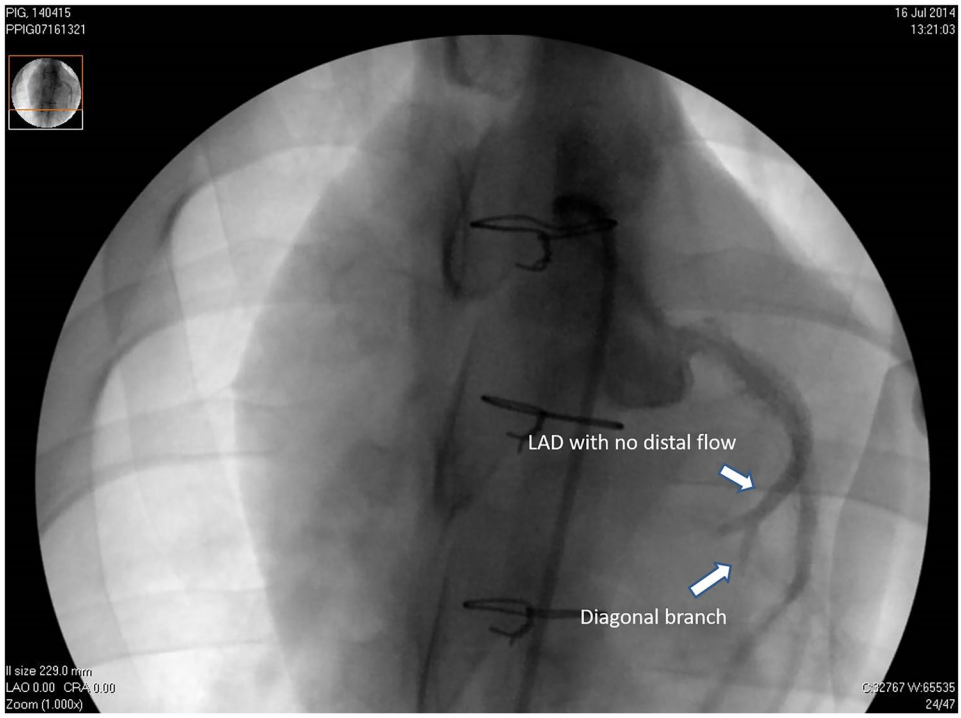

Fig. 3 This is a representative follow-up coronary angiography of a pig with the mid LAD occluded by a prolene suture. Similar imaging was performed in all six Yucatan microswine

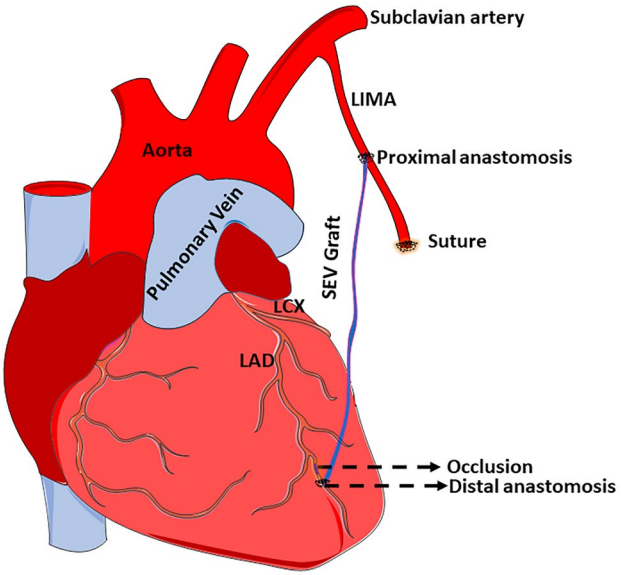

Fig. 4 Schematic illustration of the approach adopted by the study. SEV was used as bypass graft anastomosed proximally to IMA and distally to LAD. This approach was used in all six Yucatan microswine

in four out of six Yucatan microswine by grafting SEV between IMA and distal LAD (Video 1). We adopted the off-pump technique despite the technically challenging distal anastomosis on a beating heart. The 4 animals experienced no major complications during the post-operative period, suggesting the efficiency of our novel approach. Echocardiography before sacrificing the animals showed that the ejection fraction was within normal limits with no detectable wall motion abnormalities. Immediately after CABG surgery there was no significant EKG evidence of acute myocardial infarction. After comparing the preoperative, immediate postoperative and follow-up EKGs, there were no significant ST segment or Q wave variations. We performed coronary angiography and attempted to catheterize the IMA to perform graft angiography and OCT (intravascular imaging) but this was unsuccessful. After euthanasia, we opened the thoracic cavity and examined the vein graft, which appeared to be occluded by naked eye examination, and it was found to be partially or completely occluded by microscopic examination (Figs. 4–5), the operative area was infiltrated with fibro-fatty deposits (Video 2).

The technique for harvesting the vein, especially endothelial injury, triggers the pathology of graft failure which is shown to be ~ 10% greater in off-pump CABG procedures [23]. We attempted to overcome the difficulties pertaining to vein graft size by selecting the larger SEV by comparing the diameters of the veins on both sides using a superficial vascular ultrasound probe. By selecting the off-pump approach for this model, we avoided using the cardiopulmonary bypass machine, and cannulation of the anterior vena cava/the friable swine right atrium, and the inaccessible swine ascending aorta. Our strategy of feeding the animals with high fat high cholesterol diet aimed to induce hyperlipidemia and hypercholesterolemia simulating the typical

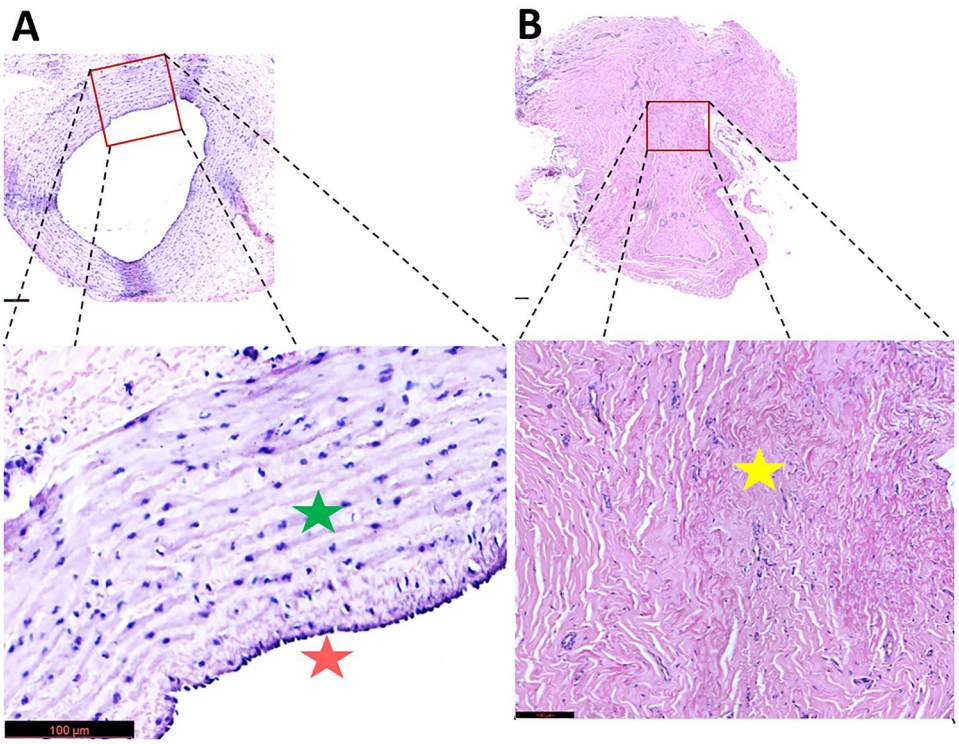

Fig. 5 A representative H and E staining of the thin section of the grafted vessel showing complete occlusion. The SEV was used as the conduit for coronary artery bypass graft. Panel (**A**) represents the SEV control harvested from an atherosclerotic pig fed with HFHC diet, and Panel (**B**) represents the post-CABG graft harvested after 6 months of surgery. The SEV control displayed intact endothelium (red star) with well-organized medial layer (green star) whereas the graft was completely occluded with fibrous tissue adhesions (black star). This is a representative of 4 Yucatan microswine

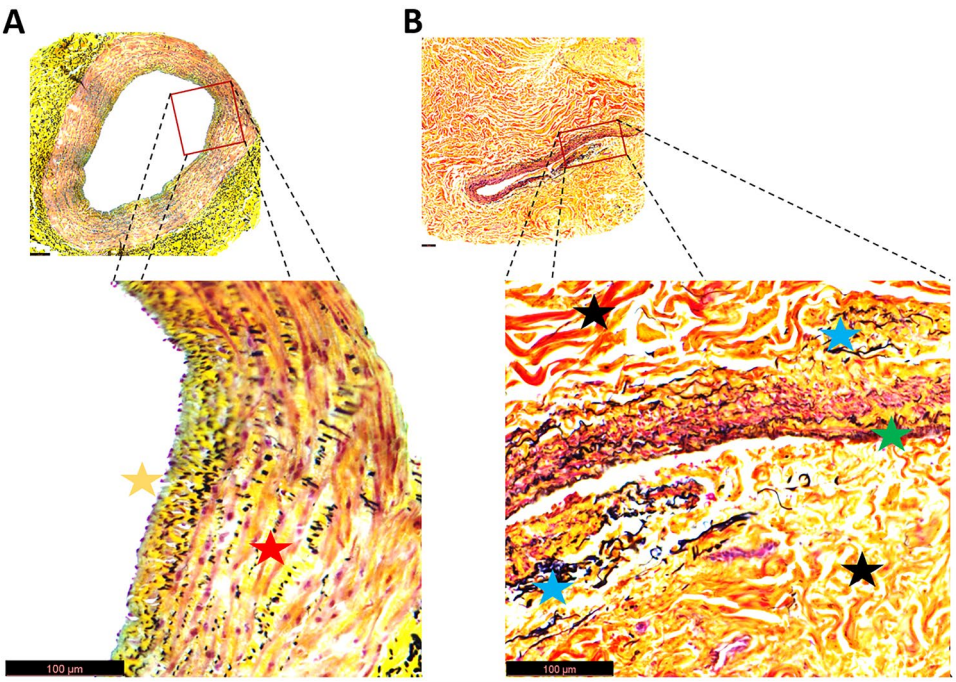

Fig. 6 A representative pentachrome staining of the thin section of the grafted vessel: the SEV used as coronary artery bypass graft. Control SEV in panel (**A**) displays intact endothelial layer (Yellow star) and medial layer (Red star) and maintenance of the vessel's structural integrity. Panel (**B**) shows severe fibrotic tissue formation as evident by the increased collagen deposition (black star) with a concomitant increase in elastic tissue (blue star). The lumen was mostly occluded with plenty of vascular smooth muscle cells (green star) in the subendothelial layer (superficial to the disrupted internal elastic membrane) suggestive of neointimal formation and proliferative smooth muscle cells which migrated from the tunica media through the disrupted internal elastic membrane. This is a representative of 4 Yucatan microswine

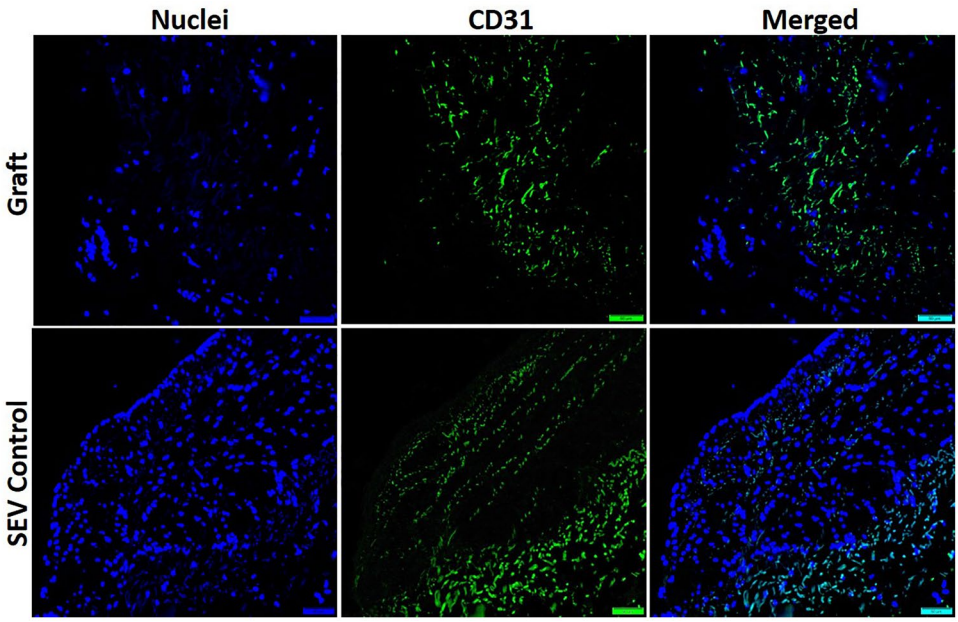

Fig. 7 Immunofluorescence analysis for the expression of CD31 in the graft and SEV control. Images in the top row are histological sections of graft and SEV control (second row) Images in the left column show nuclear staining with DAPI; the images in the middle column show expression of CD31 while the images in the right column show overlay of CD31 with DAPI. Images were acquired at 20× magnification

clinical scenario of CAD patients and to potentially determine the effects of hyperlipidemia and hypercholesterolemia on the vein graft patency.

In the initial CABG surgeries on domestic swine, we encountered high mortality rate due to persistent hypotension and intractable bleeding, as it was challenging to expose the ascending aorta and to perform the side to end aorto-venous anastomosis. Consequently, we decided to use the IMA instead of the ascending aorta for the proximal anastomosis. To avoid occluding the proximal LAD, which exposes a great portion of the left ventricular myocardium to ischemia (Fig. 3), with a higher incidence of fatal refractory VF, we decided to perform the Coronary- venous anastomosis as distal as possible in the LAD.

The disorganized ECM and excess collagen deposition are the major hallmarks of fibrotic events which was vivid in the histological examination of post-CABG graft (Fig. 5). Data from the controlled clinical trials demonstrated more than 30–40% vein graft occlusion or stenosis develop within 5 years of surgery. The remodeling responses in the vein graft are intimately impacted by the sustained inflammation resulting in cellular apoptosis and impaired ECM turnover. Hence, the dramatic alterations in the physical, physiological, and biomechanical are obvious in the arterialized vein subsequently occluding the lumen [24] [25]. The altered ECM homeostasis has been attributed to the hyperactivation of MMPs accelerating the downstream signaling resulting in fibrosis as evident from the rabbit vein graft model [26]. Similar observation has been reported in human SVG pathology. Min et al. [18] demonstrated physiological and biochemical similarities of SEV in the swine model for CABG suggesting a similar histological features post-CABG. However, the information regarding the comparative analysis of human SVG and swine SEV for CABG applications is unavailable in the literature warranting further investigations. Moreover, the molecular pathology underlying the fibrotic reactions in vein graft failure requires further attention.

Advantages of the swine model

Swine model of CABG exhibits many advantages. The swine coronary vasculature, myocardial oxygen consumption, and metabolic patterns are similar to human [27, 28]. The Yucatan microswine develops spontaneous atherosclerosis especially on feeding with a high cholesterol diet, ensuring the simulation of the human pathological features of coronary artery disease (CAD) [29, 30]. The surgical, interventional, and imaging techniques, tools and equipment used in this model are like those used clinically in patients.

Disadvantages of the swine model and limitations of the study

The swine model exhibits a narrow acoustic window due to the thickness and orientation of the thoracic cage, which limits the echocardiographic assessment of the left ventricle wall [31]. In the Yucatan microswine model, we could not achieve successful angiography and OCT imaging of the graft due to the difficult catheterization of the IMA. The incidence of vein graft failure has been reported to be higher in off-pump compared to the traditional on-pump CABG, which represents a confounding factor for studying the vein graft disease in this model. Lack of an experimental group of microswine on a normal

diet limited our ability to study the effect of hypercholesterolemia on the vein graft patency Despite these limitations, this swine model represents a promising translational model of vein-graft disease, which is sustainable and reproducible to explore the underlying pathophysiology and test better therapeutic approaches of vein graft disease.

Conclusions

We report the novel swine model of CABG using SEV as a conduit. The swine SEV was effectively used as an analogue of the saphenous vein graft in humans. The SEV grafts were partially or completely occluded after 10 months following the off-pump CABG procedure. This model represents the vein graft failure associated with the human CABG procedure. It offers a translational platform to investigate the underlying molecular and pathologic mechanisms of vein graft disease, and to develop innovative therapeutic strategies to prevent it.

Supplementary Information The online version contains supplementary material available at https://doi.org/10.1007/s11748-021-01725-y.

Acknowledgements The authors acknowledge the support of several individuals during the initial stages of establishing the CABG model in swine. These individuals include: Gunasekar Palanikumar MBBS, Liang Mo MD, Jubing Zhang MD, Zefu Zhang MD, Marcus Balters MD, Ashok Kujur MSc, Michael J. Moulton MD, and several veterinary technicians.

Funding The research work of DK Agrawal is supported by research grants R01HL 128063, R01 HL144125 and R01HL147662 from the National Institutes of Health, USA. The content of this review article is solely the responsibility of the authors and does not necessarily represent the official views of the National Institutes of Health.

Declarations

Conflict of interest All authors have read the journal's policy on disclosure of potential conflicts of interest. Author E (DKA) has received grants from the National Institutes of Health. Other authors (MMR, AS, FGT, KTK) have no relevant affiliations or financial or non-financial involvement with any organization or entity with financial or non-financial interest or conflict with the subject matter or materials discussed in the manuscript apart from those disclosed. All authors (MMR, AS, FGT, KTK, DKA) declare that they have no conflict of interest.

Ethical approval All institutional and national guidelines for the care and use of laboratory animals were followed and approved by the appropriate institutional committees.

References

1. Safaie N, Montazerghaem H, Jodati A, Maghamipour N. In-Hospital complications of coronary artery bypass graft surgery in patients older than 70 years. J Cardiovasc Thorac Res. 2015;7:60–2.
2. Velazquez EJ, Lee KL, Jones RH, Al-Khalidi HR, Hill JA, Panza JA, et al. Coronary-artery bypass surgery in patients with ischemic cardiomyopathy. N Engl J Med. 2016;374:1511–20.
3. ter Woorst JF, van Straten AHM, Houterman S, Soliman-Hamad MA. Sex Difference in coronary artery bypass grafting: preoperative profile and early outcome. J Cardiothorac Vasc Anesth. 2019;33:2679–84.
4. Dianati Maleki N, Ehteshami Afshar A, Parikh PB. Management of saphenous vein graft disease in patients with prior coronary artery bypass surgery. Curr Treat Options Cardiovasc Med [Internet]. 2019 [cited 2019 Apr 5];21. Available from: http://link.springer.com/https://doi.org/10.1007/s11936-019-0714-7
5. Hosono M, Murakami T, Hirai H, Sasaki Y, Suehiro S, Shibata T. The risk factor analysis for the late graft failure of radial artery graft in coronary artery bypass grafting. Ann Thorac Cardiovasc Surg. 2019;25:32–8.
6. Maznyczka AM, Barakat MF, Ussen B, Kaura A, Abu-Own H, Jouhra F, et al. Calculated plasma volume status and outcomes in patients undergoing coronary bypass graft surgery. Heart. 2019; heartjnl-2018-314246.
7. Prim DA, Zhou B, Hartstone-Rose A, Uline MJ, Shazly T, Eberth JF. A mechanical argument for the differential performance of coronary artery grafts. J Mech Behav Biomed Mater. 2016;54:93–105.
8. Possati G, Gaudino M, Prati F, Alessandrini F, Trani C, Glieca F, et al. Long-term results of the radial artery used for myocardial revascularization. Circulation. 2003;108:1350–4.
9. Thankam FG, Ayoub JG, Ahmed MMR, Siddique A, Sanchez TC, Peralta RA, et al. Association of hypoxia and mitochondrial damage associated molecular patterns in the pathogenesis of vein graft failure: a pilot study. Transl Res. 2021;229:38–52.
10. Chandrasekhar SK, Thankam FG, Agrawal DK, Ouseph JC. 2-Interface biology of stem cell–driven tissue engineering: concepts, concerns, and approaches. In: Sharma CP, editor. Biointegration Med Implant Mater Second Edn [Internet]. Woodhead Publishing; 2020 [cited 2019 Oct 15]. p. 19–44. Available from: http://www.sciencedirect.com/science/article/pii/B9780081026809000020
11. Duffield JS, Lupher M, Thannickal VJ, Wynn TA. Host responses in tissue repair and fibrosis. Annu Rev Pathol Mech Dis. 2013;8:241–76.
12. Thankam FG, Roesch ZK, Dilisio MF, Radwan MM, Kovilam A, Gross RM, et al. Association of inflammatory responses and ECM disorganization with HMGB1 upregulation and NLRP3 inflammasome activation in the injured rotator cuff tendon. Sci Rep. 2018;8:1–14.
13. Thankam FG, Boosani CS, Dilisio MF, Dietz NE, Agrawal DK. MicroRNAs associated with shoulder tendon matrisome disorganization in glenohumeral arthritis. PLoS ONE. 2016;11:e0168077.
14. Thankam FG, Dilisio MF, Dietz NE, Agrawal DK. TREM-1, HMGB1 and RAGE in the shoulder tendon: dual mechanisms for inflammation based on the coincidence of glenohumeral arthritis. PLoS ONE. 2016;11:e0165492.
15. Almeida JI, Javier JJ, Mackay E, Bautista C, Proebstle TM. First human use of cyanoacrylate adhesive for treatment of saphenous vein incompetence. J Vasc Surg Venous Lymphat Disord. 2013;1:174–80.
16. Cable DG, Dearani JA, Pfeifer EA, Daly RC, Schaff HV. Minimally invasive saphenous vein harvesting: endothelial integrity and early clinical results11This article has been selected for the open discussion forum on the STS Web site: http://www.sts.org/annals. Ann Thorac Surg. 1998;66: 139–43.
17. Coupland A, Stansby G. Glue for superficial venous ablation. Rev Vasc Med. 2014;2:98–102.
18. Min RJ, Almeida JI, Mclean DJ, Madsen M, Raabe R. Novel vein closure procedure using a proprietary cyanoacrylate

adhesive: 30-day swine model results. Phlebol J Venous Dis. 2012;27:398–403.
19. Radak D, Djukic N, Neskovic M. Cyanoacrylate embolization: a novelty in the field of varicose veins surgery. Ann Vasc Surg. 2019;55:285–91.
20. Rojas-Pena A, Koch KL, Heitner HD, Hall CM, Bergin IL, Cook KE. Quantification of thermal spread and burst pressure after endoscopic vessel harvesting: a comparison of 2 commercially available devices. J Thorac Cardiovasc Surg. 2011;142:203–8.
21. Schachner T, Laufer G, Bonatti J. In vivo (animal) models of vein graft disease☆. Eur J Cardiothorac Surg [Internet]. 2006 [cited 2019 Aug 16]; 30: 451–63. https://doi.org/10.1016/j.ejcts.2006.06.015
22. Wang D, Tediashvili G, Pecha S, Reichenspurner H, Deuse T, Schrepfer S. Vein interposition model: a suitable model to study bypass graft patency. J Vis Exp. 2017;2017:54839.
23. Laflamme M, DeMey N, Bouchard D, Carrier M, Demers P, Pellerin M, et al. Management of early postoperative coronary artery bypass graft failure. Interact Cardiovasc Thorac Surg [Internet]. 2012 [cited 2019 Aug 16]; 14: 452–6. https://doi.org/10.1093/icvts/ivr127
24. Owens CD, Gasper WJ, Rahman AS, Conte MS. Vein graft failure. J Vasc Surg. 2015;61:203–16.
25. Owens CD, Rybicki FJ, Wake N, Schanzer A, Mitsouras D, Gerhard-Herman MD, et al. Early remodeling of lower extremity vein grafts: inflammation influences biomechanical adaptation. J Vasc Surg. 2008;47:1235–42.
26. Jiang Z, Tao M, Omalley KA, Wang D, Ozaki CK, Berceli SA. Established neointimal hyperplasia in vein grafts expands via TGF-beta-mediated progressive fibrosis. Am J Physiol Heart Circ Physiol. 2009;297:H1200-1207.
27. Hocum Stone L, Butterick TA, Duffy C, Swingen C, Ward HB, Kelly RF, et al. Cardiac strain in a swine model of regional hibernating myocardium: effects of CoQ10 on contractile reserve following bypass surgery. J Cardiovasc Transl Res. 2016;9:368–73.
28. Litten-Brown JC, Corson AM, Clarke L. Porcine models for the metabolic syndrome, digestive and bone disorders: a general overview. Animal. 2010;4:899–920.
29. Li S-J, Liu C-H, Chang C-W, Chu H-P, Chen K-J, Mersmann HJ, et al. Development of a dietary-induced metabolic syndrome model using miniature pigs involvement of AMPK and SIRT1. Eur J Clin Invest. 2015;45:70–80.
30. Turk JR, Henderson KK, Vanvickle GD, Watkins J, Laughlin MH. Arterial endothelial function in a porcine model of early stage atherosclerotic vascular disease: Minipig model of endothelial dysfunction. Int J Exp Pathol. 2005;86:335–45.
31. Hocum Stone LL, Swingen C, Holley C, Wright C, Chappuis E, Ward HB, et al. Magnetic resonance imaging assessment of cardiac function in a swine model of hibernating myocardium 3 months following bypass surgery. J Thorac Cardiovasc Surg. 2017;153:582–90.